Mathematical Biosciences and Engineering

MBE, 19 (6): 6362–6378.
DOI: 10.3934/mbe.2022298
Received: 29 January 2022
Revised: 13 March 2022
Accepted: 05 April 2022
Published: 22 April 2022

http://www.aimspress.com/journal/MBE

Research article

Sliding-mode controller synthesis of robotic manipulator based on a new modified reaching law

Xinyu Shao[1], Zhen Liu[1,2,*] and Baoping Jiang[3,*]

[1] School of Automation, Qingdao University, Qingdao 266071, China
[2] Shandong Key Laboratory of Industrial Control Technology, Qingdao University, Qingdao 266071, China
[3] School of Electronic and Information Engineering, Suzhou University of Science and Technology, Suzhou 215000, China

* **Correspondence:** Email: zliu@qdu.edu.cn; baopingj@163.com.

Abstract: In this study, an adaptive modified reaching law-based switch controller design was developed for robotic manipulator systems using the disturbance observer (DO) approach. Firstly, a standard DO is employed to estimate the unknown disturbances of the plant, from which the control signal could be compensated. Then, an adaptive modified reaching law is established to dynamically adapt the switching gain of the sliding mode robust term and further guarantee the finite-time arrival of the established sliding surface. Additionally, the convergence of the error system is analyzed via the Lyapunov method. At last, the feasibility and effectiveness of the proposed control scheme are verified by using a two-joint robotic manipulator model. The simulation results show that the developed controller can achieve rapid tracking, reduce system chattering and improve the robustness of the plant. The main innovations of the work are as follows. 1) A new adaptive reaching law is proposed; it can reduce chattering effectively, and it has a fast convergence speed. 2) Regarding the nonlinear robotic manipulator model, a novel adaptive sliding-mode controller was synthesized based on the DO to estimate the unknown disturbance and ensure effective tracking of the desired trajectory.

Keywords: robotic manipulator; sliding-mode controller; modified reaching law; disturbance observer; Lyapunov method

1. Introduction

In general, highly nonlinear characteristics exist in many practical plants, such as the manipulator. At present, robotic manipulators are widely used in mechanical manufacturing, medical treatment, space exploration, disaster rescue and other dangerous or high-precision scenes. As a result, it is critical to investigate manipulator tracking control at high speeds, and with high precision [1–4]. Due to modeling errors, external disturbances, etc., achieving control of the manipulator plant is a difficult task [5–7]. Sliding-mode control (SMC), as a typical robust control strategy [8–11], has the potential merits of simple structure, good adaptability and high robustness in the face of unknown nonlinear uncertainties [12–15], which are also extensively applied to the manipulator.

Considering the tracking problem of robotic manipulator models, different control schemes have been put forward, such as backstepping control [16], neural network control [17], and SMC [18–21]. In [17], a new model-free neural network was presented; it could solve the learning-based control issue of a manipulator in a unified framework. In [18], a systematic approach to nonlinear disturbance observer (NDO) development was presented, and the NDO was utilized to design a computed-torque controller. A finite-time control strategy based on terminal SMC was proposed for the manipulator in [19]. In [20], based on time-delay estimation, a novel adaptive SMC scheme was developed, and the proposed adaptive SMC algorithm could achieve good tracking and reduce the chattering of the plant.

As seen, trajectory tracking control can be effectively achieved for the robotic manipulator via SMC [21]. However, there exists chattering near the equilibrium point of the system. It should be noted that severe chattering will degrade the system's performance. As such, the reaching law method is a common way to reduce chattering [22], as it can improve the dynamic performance of the system during the reaching phase of the sliding surface (SS) and alleviate the high-frequency chattering. Taking the exponential reaching law as an example, the exponential term ensures that the system state can approach to SS quickly when it is far away from the SS. While the state is close to the SS, the reaching speed will be decided mainly by the constant-rate term, which ensures the limited-moment reachability of the SS as expected.

In past years, a great amount of effort to modify the reaching law approach has been put forth by numerous scholars. Regarding permanent magnet synchronous motor control in [23], a new exponential reaching law (NERL) was proposed to improve the dynamic performance, where the NERL could reduce the chattering and accelerate the reaching speed of the SS. However, it is noted that, as system states become close to the equilibrium point, the effects of the NERL on the convergence and robustness of the system will be weaken. Thus, a novel reaching law (NRL) was provided in [24]; it decreased the reaching speed while approaching the SS, and the SMC applied to a 2-DOF (degrees of freedom) manipulator system was developed based on the NRL. Namely, if the system states are not located near the SS, the speed of the reaching phase according to the NRL is relatively slow; moreover, since the bounds of the switching gain are fixed, the reaching speed can not be updated dynamically; this further results in a longer reaching time and the degradation of the system performance to some degree. To this end, chattering reduction has always been an important control issue for the manipulator with SMC; the problem of how to further improve the reaching law-based MC method is still meaningful and open, and has thus formed the motivation of this study.

On the basis of the aforementioned studies, a novel adaptive control scheme for robotic manipulator dynamic models was developed in this study. The main contributions can be summarized as follows:

(1) An adaptive modified reaching law is provided; it can dynamically adjust the change of the sliding function (SF), accelerate the convergence speed and reduce the chattering to some extent.

(2) The devised switching gain is an adaptive value for the improvement of the control properties, and the novel adaptive SMC was designed for system tracking in conjunction with the disturbance observer (DO) to estimate the disturbance input; the hyperbolic tangent function is employed to make the control input smooth and weaken the chattering further.

(3) The proposed control scheme achieved the expected performance in simulation experiments; its advantage was further verified and analyzed from the transient and steady performance of the plant.

2. Dynamic model of robotic manipulators

Taking the external disturbance and modeling error into consideration, an *n*-DOF robotic manipulator dynamic model is given by

$$M(q)\ddot{q}+C(q,\dot{q})\dot{q}+G(q)=u+d\,, \tag{1}$$

where $q,\dot{q},\ddot{q}\in R^n$ represent the position vector, velocity vector and acceleration vector, respectively. $M(q)\in R^{n\times n}$ stands for the positive definite inertia matrix of the plant; $C(q,\dot{q})\in R^{n\times n}$ denotes the Coriolis-centripetal matrix; the gravitational torque vector is expressed as $G(q)\in R^n$; u and d are the control input vector and external disturbance, respectively. Generally, an accurate dynamic model of the manipulator during the actual control process may be difficult to solve; then, $M(q)$, $C(q,\dot{q})$ and $G(q)$ are assumed to be as follows:

$$\begin{cases} M(q)=M_0(q)+\delta M(q) \\ C(q,\dot{q})=C_0(q,\dot{q})+\delta C(q,\dot{q}) \\ G(q)=G_0(q)+\delta G(q) \end{cases}, \tag{2}$$

where $M_0(q)$, $C_0(q,\dot{q})$ and $G_0(q)$ are the nominal values, and $\delta M(q)$, $\delta C(q,\dot{q})$ and $\delta G(q)$ are the parameter differences between the nominal values and the actual values. Therefore, the dynamics of the robotic manipulator (1) can be expressed as

$$M_0(q)\ddot{q}+C_0(q,\dot{q})\dot{q}+G_0(q)=u+d+\delta_\Delta\,, \tag{3}$$

where $\delta_\Delta=-\delta M(q)\ddot{q}-\delta C(q,\dot{q})\dot{q}-\delta G(q)$ represents the unknown uncertainties. Defining $x=[x_1 \quad x_2]^T$, where $x_1=q$ and $x_2=\dot{q}$, the dynamical equation of the plant can be written as

$$\begin{cases} \dot{x}_1=x_2, \\ \dot{x}_2=Q(x)+P(x)u+F(t,x) \end{cases}, \tag{4}$$

where $Q(x)=-M_0^{-1}(q)C_0(q,\dot{q})-M_0^{-1}(q)G_0(q)$, $P(x)=M_0^{-1}(q)$ and $F(t,x)=M_0^{-1}(q)(d+\delta_\Delta)$; $F(t,x)$ is a lumped disturbance. In the position, the tracking error vector is then expressed as

$$\begin{cases} e_1=x_1-x_{1d} \\ e_2=x_2-x_{2d} \\ e_2=\dot{e}_1 \end{cases}, \tag{5}$$

where $x_{1d}, x_{2d} \in R^n$ are, respectively, the desired angular position and angular velocity. As can be seen, Figure 1 shows a two-joint manipulator model.

Lemma 1 [25]. Suppose that $V(x)$ is a smooth positive definite function defined on $D \subset R^n$; it satisfies $\dot{V}(x) + \mu V^{\eta}(x) \leq 0, \mu > 0, \eta \in (0,1)$, where μ and η are two positive constants. Then, for any specified t_0, there exists an area $D_0 \subset R^n$ such that $V(x)$, which starts from D_0, can be $V(x) \equiv 0$ in finite time; moreover, the settling time t_r satisfies $t_r \leq \dfrac{V^{1-\eta}(t_0)}{\mu(1-\eta)}$.

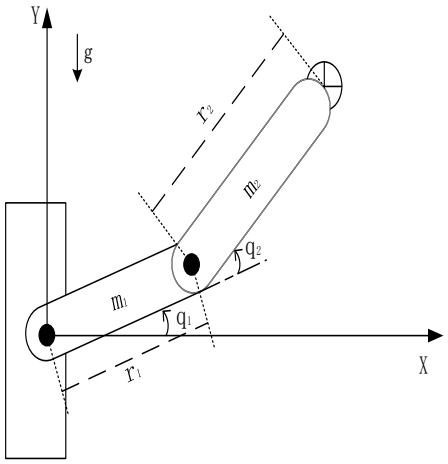

Figure 1. Two-joint robotic manipulator.

3. Design of DO

According to the dynamics described by Eq. (4), we have

$$F(t,x) = \dot{x}_2 - Q(x) - P(x)u. \tag{6}$$

Hereafter, we refer to $\hat{F}(t,x)$ as the estimated value of the lumped disturbance. The aim is focused on correcting the difference between the estimated output and the actual output. Then, the basic DO can be written as

$$\dot{\hat{F}}(t,x) = K[F(t,x) - \hat{F}(t,x)]. \tag{7}$$

By substituting Eq. (6) into Eq. (7), the following can be obtained:

$$\dot{\hat{F}}(t,x) = -K\hat{F}(t,x) + K[\dot{x}_2 - Q(x) - P(x)u]. \tag{8}$$

However, due to the observation noise in practice, it is not easy to obtain the acceleration signal by differentiating the velocity signal directly. For the robotic manipulators, it is also difficult to obtain the actual acceleration signal. Thus, we also introduce an auxiliary variable, as shown below.

$$z = \hat{F}(t,x) - Kx_2. \tag{9}$$

By combining Eq. (4) and Eq. (9), it can be obtained that

$$\dot{z} = \dot{\hat{F}}(t,x) - K\dot{x}_2 = -K\hat{F}(t,x) + K[-Q(x) - P(x)u]. \tag{10}$$

Then, the devised DO is given as

$$\begin{cases} \dot{z} = -K[Q(x) + P(x)u] - K\hat{F}(t,x) \\ \hat{F}(t,x) = z + Kx_2 \end{cases}, \tag{11}$$

in which the observation error $\tilde{F}(t,x)$ is defined as

$$\tilde{F}(t,x) = F(t,x) - \hat{F}(t,x). \tag{12}$$

Lemma 2 [26]. Considering the dynamics described by Eq. (4), the DO in Eq. (11) guarantees that the observation error $\tilde{F}(t,x)$ will converge to zero.

As can be observed, the DO does not need the information on the acceleration signal. The disturbance observation error can converge as expected, and the convergence accuracy is determined by K.

4. Design of adaptive switch controller

In this section, by applying the provided DO and updating law, a new modified reaching law-based adaptive switch controller was synthesized to improve the dynamic performance of trajectory tracking and reduce the chattering; the control structure of the plant is shown in Figure 2.

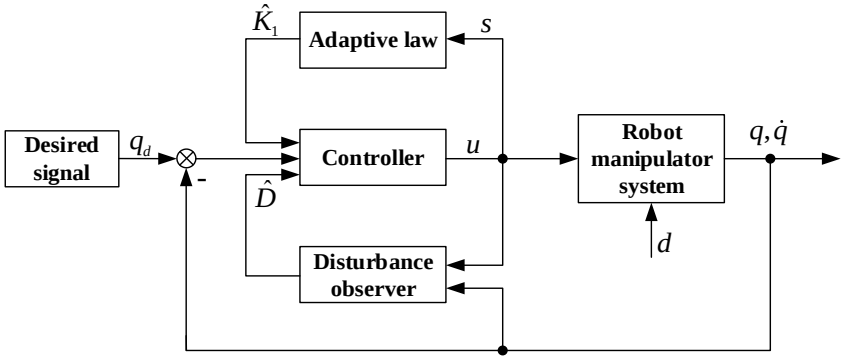

Figure 2. System control structure diagram.

4.1. Development of modified reaching law

As is known, the reaching law strategy is extensively employed for SMC designs for manipulator systems, allowing them to achieves the dynamic performance of the reaching stage. A proper reaching law allows the system trajectories to reach the SS fast, and with low chattering. Firstly, the following Eq. (13) is the traditional constant-rate reaching law [22]:

$$\dot{s} = -k\text{sgn}(s), k > 0. \tag{13}$$

Remark 1. It should be mentioned that the constant-rate reaching law in [22] results in a longer reaching time and more chattering. In [24], an NRL was also developed using the constant-rate

reaching law approach; it could shorten the reaching time and reduce the chattering. A new modified adaptive reaching law has been established based on the NRL method by combining the adaptive method described in this paper to better alleviate the adverse factors of chattering and further speed up the tracking convergence.

The following is the proposed reaching law:

$$\dot{s} = -(\frac{K_1}{N(s)} + \partial_1)\,\mathrm{sgn}(s) - \phi(1-e^{-\lambda|s|})s, K_1 > 0, \tag{14}$$

where $N(s) = \partial_0 + (1+1/|s|^{\theta} - \partial_0)e^{-\varepsilon|s|^p}$, $\partial_0 \in (0,1)$, p is a positive integer, $\varepsilon, \phi, \lambda > 0$ and $\theta \in (0,1)$. K_1 is a part of the controller that, together with $N(s)$ and ∂_1, forms the switching gain; $\frac{K_1}{\partial_0} + \partial_1$ is the upper bound of the switching gain. ∂_1 is a small positive constant used to prove the reachability of the designed SS in finite time.

Remark 2. As can be ascertained from the reaching law presented in Eq. (14), $N(s)$ will tend to ∂_0 with increasing $|s|$; then, it has $\frac{K_1}{N(s)} > K_1$, and $\phi(1-e^{-\lambda|s|})$ becomes ϕ. The system state will then approach the SS at a faster speed; in a like manner, as $|s|$ decreases, $N(s)$ will tend toward $1+1/|s|^{\theta}$, which is much bigger than 1. Thus, it follows that $\frac{K_1}{N(s)}$ K_1. Also, $\phi(1-e^{-\lambda|s|})$ will approach zero, and $\frac{K_1}{N(s)} + \partial_1$ will gradually decrease to a small value.

4.2. SMC law synthesis

The SF is selected as follows:

$$s = e_2 + ce_1. \tag{15}$$

In view of Eq. (5) and Eq. (15), the derivative of SF can be obtained as

$$\dot{s} = \dot{e}_2 + c\dot{e}_1 = \dot{x}_2 - \dot{x}_{2d} + c\dot{e}_1. \tag{16}$$

Remark 3. In view of the modified reaching law given in Eq. (14), the parameter K_1 is presented as an unknown quantity that will be estimated by the adjusting parameter $\hat{K}_1$, which aims to change the convergence speed and further improve the control performance. Moreover, the boundary layer method is widely used for chattering reduction in SMC; the SF will not exactly reach zero, but it will arrive at a small vicinity of zero point because measurement noise and switching delay/imperfections may often occur in practice. Then, the following adaptive law with a small positive constant σ_0 is provided to avoid the infinite increase of the switching gain, as described below. (Here, σ_0 is set by a user based on the simulation results to control the effects in practical applications.)

$$\dot{\hat{K}}_1 = \begin{cases} \dfrac{\xi|s|}{N(s)} & s > \sigma_0 \\ 0 & s \le \sigma_0 \end{cases}, \tag{17}$$

where σ_0 is a small positive constant. Here, $\tilde{K}_1$ is the estimation error between K_1 and $\hat{K}_1$, which is defined as

$$\tilde{K}_1 = \hat{K}_1 - K_1. \tag{18}$$

Assumption 1. The estimation error of the DO is bounded and satisfies

$$\frac{K_1}{N(s)} \ge \left|\tilde{F}(t,x)\right|. \tag{19}$$

According to Eq. (4), the devised adaptive switch controller for the considered manipulator plant, which was developed based on the proposed reaching law, is given as follows:

$$u_{eq} = P^{-1}(x)[-Q(x) + \dot{x}_{2d} - c\dot{e}_1], \tag{20}$$

$$u_{sw} = P^{-1}(x)[-(\frac{\hat{K}_1}{N(s)} + \partial_1)\mathrm{sgn}(s) - \phi(1 - e^{-\lambda|s|})s - \hat{F}(t,x)], \tag{21}$$

$$u = u_{eq} + u_{sw} = P^{-1}(x)[-(\frac{\hat{K}_1}{N(s)} + \partial_1)\mathrm{sgn}(s) - \phi(1 - e^{-\lambda|s|})s - Q(x) - \hat{P}(t,x) + \dot{x}_{2d} - c\dot{e}_1]. \tag{22}$$

Theorem 1. Considering the adaptive law in Eq. (17), if the control law in Eq. (22) is applied to the system in combination with the DO in Eq. (11), the SF will approach zero in finite moments; then, the trajectory tracking error will converge to zero.

Proof. Consider the Lyapunov function as below.

$$V_1 = \frac{1}{2}s^2 + \frac{1}{2\xi}\tilde{K}_1^{\,2}. \tag{23}$$

Given Eq. (4), Eq. (16) and Eq. (22), the derivative of Eq. (23) is expressed as

$$\begin{aligned}\dot{V}_1 &= s\dot{s} + \frac{1}{\xi}\tilde{K}_1\dot{\tilde{K}}_1 \\ &= s[\dot{x}_2 - \dot{x}_{2d} + c\dot{e}_1] + \frac{1}{\xi}\tilde{K}_1\dot{\tilde{K}}_1 \\ &= s[Q(x) + P(x)u + F(t,x) - \dot{x}_{2d} + c\dot{e}_1] + \frac{1}{\xi}\tilde{K}_1\dot{\tilde{K}}_1 \\ &= s[F(t,x) - \hat{F}(t,x) - (\frac{\hat{K}_1}{N(s)} + \partial_1)\mathrm{sgn}(s) - \phi(1-e^{-\lambda|s|})s] + \frac{1}{\xi}\tilde{K}_1\dot{\tilde{K}}_1 \\ &= s[\tilde{F}(t,x) - (\frac{\hat{K}_1}{N(s)} + \partial_1)\mathrm{sgn}(s) - \phi(1-e^{-\lambda|s|})s] + \frac{1}{\xi}\tilde{K}_1\dot{\tilde{K}}_1 \\ &= \tilde{F}(t,x)s - (\frac{\hat{K}_1}{N(s)} + \partial_1)|s| - \phi(1-e^{-\lambda|s|})s^2 + \frac{1}{\xi}\tilde{K}_1\dot{\tilde{K}}_1\end{aligned} \tag{24}$$

By substituting the adaptive law of Eq. (17), it follows that

$$\begin{aligned}\dot{V}_1 &= \tilde{F}(t,x)s - (\frac{K_1}{N(s)} + \partial_1)|s| - \phi(1-e^{-\lambda|s|})s^2 + \tilde{K}_1(\frac{1}{\xi}\dot{\tilde{K}}_1 - \frac{|s|}{N(s)}) \\ &\le -(\frac{K_1}{N(s)} - \tilde{F}(t,x))|s| - \partial_1|s| \\ &\le -\partial_1|s|.\end{aligned} \tag{25}$$

Since $\dot{\tilde{K}}_1 > 0\ (s > \sigma_0)$, there exists an instant T, and for any $t > T$, one has $\tilde{K}_1 \ge 0$; thus, it follows that $\frac{1}{\xi}\tilde{K}_1\dot{\tilde{K}}_1 \ge 0$. Let

$$V = 0.5s^2. \tag{26}$$

It can be obtained that

$$\dot{V} \le -\sqrt{2}\partial_1 V^{0.5}. \tag{27}$$

From Lemma 1, the reaching time can be estimated as $t_r \le \frac{\sqrt{2}}{\partial_1}V^{0.5}(0)$. Namely, the SF will equal zero in finite time. Due to the condition $s = 0$, it follows that e_1 and e_2 have opposite signs. Therefore, the tracking error will converge to zero. The proof is finished.

Remark 4 [27]. The signum function in the designed controller could be approximated by the hyperbolic tangent function described by Eq. (28) to make the switched control input continuous, and to further reduce the chattering of the plant.

$$\tanh(\Lambda s_i) = \frac{e^{\Lambda s_i} - e^{-\Lambda s_i}}{e^{\Lambda s_i} + e^{-\Lambda s_i}}, \tag{28}$$

where $\Lambda > 0$ is a constant, and $\frac{1}{\Lambda}$ is the boundary layer.

5. Simulation results

The simulations of a 2-DOF robotic manipulator were carried out to verify the advantages and feasibility of the presented controller design. The dynamic model of the manipulator is expressed as

$$\begin{bmatrix} m_{11} & m_{12} \\ m_{21} & m_{22} \end{bmatrix} \begin{bmatrix} \ddot{q}_1 \\ \ddot{q}_2 \end{bmatrix} + \begin{bmatrix} c_{11} & c_{12} \\ c_{21} & c_{22} \end{bmatrix} \begin{bmatrix} \dot{q}_1 \\ \dot{q}_2 \end{bmatrix} + \begin{bmatrix} g_1 \\ g_2 \end{bmatrix} = u + d, \tag{29}$$

where $m_{11} = (m_1 + m_2)r_2^2 + 2m_2 r_1 r_2 \cos q_2 + j_1$; $m_{12} = m_2 r_2^2 + m_2 r_1 r_2 \cos q_2$; $m_{21} = m_{12}$; $m_{22} = m_2 r_2^2 + j_2$; $c_{11} = -m_2 r_1 r_2 \sin(q_2)\dot{q}_1$; $c_{12} = -2m_2 r_1 r_2 \sin(q_2)\dot{q}_1$; $c_{21} = 0$; $c_{22} = m_2 r_1 r_2 \sin(q_2)\dot{q}_2$; $g_1 = [(m_1 + m_2)r_1 \cos q_2 + m_2 r_2 \cos(q_1 + q_2)]g$; $g_2 = m_2 r_2 g \cos(q_1 + q_2)$.

For the simulation, the physical parameters of the manipulator described by Eq. (29) were set as $m_1 = 0.5\text{kg}$, $m_2 = 1.5\text{kg}$, $r_1 = 1\text{kg}$, $r_2 = 0.5\text{kg}$, $g = 9.8\text{N/kg}$ and $j_1 = j_2 = 5\text{kg}\cdot\text{m}$. Assume that the initial position $q_0 = [2 \quad 3]^T$ and initial velocity $\dot{q}_0 = [0 \quad 0]^T$ of the plant were set in advance.

Suppose that the plant uncertainties are $\delta M(q) = -0.2M_0(q)$, $\delta C(q,\dot{q}) = -0.2C_0(q,\dot{q})$ and $\delta G(q) = -0.2G_0(q)$. The external disturbance is supposed to be $d = [18\cos(\pi t), 10\sin(\pi t)]^T$. The simulation results obtained using the devised controller described by Eq. (22), which had the parameters $c = 3$, $K = 40$, $\partial_0 = 0.5$, $\theta = 0.1$, $\varepsilon = 1$, $p = 1$, $\lambda = 1.6$, $\phi = 5$, $\Lambda = 70$, $\partial_1 = 0.001$ and $\xi = 2.5$, are depicted in Figures 3–5. The goal was to control the manipulator joint to effectively follow the desired trajectory $q_d = [1.25 - 1.4e^{-t} + 0.35e^{-4t} \quad 1.25 + e^{-t} - 0.25e^{-4t}]^T$.

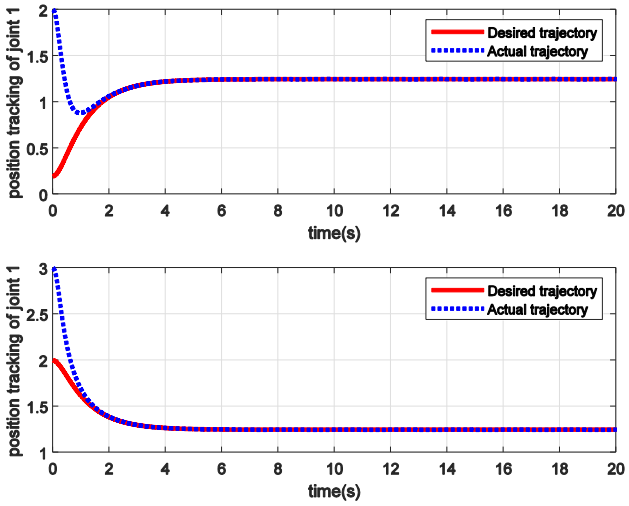

Figure 3. Two-joint trajectory tracking.

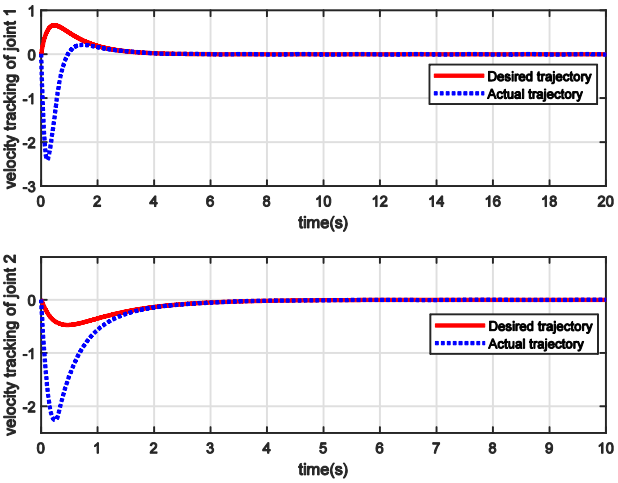

Figure 4. Two-joint velocity tracking.

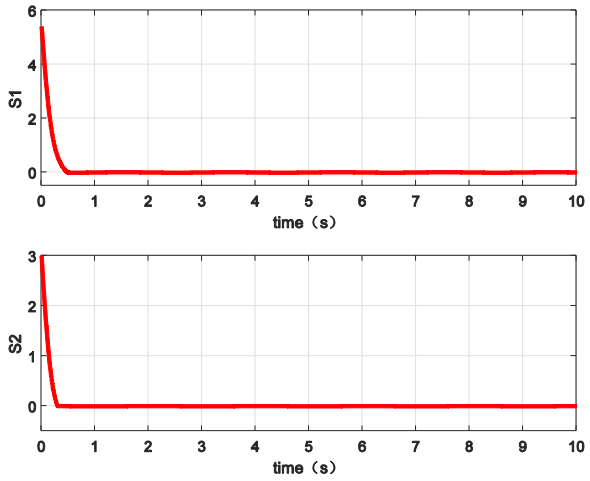

Figure 5. SFs.

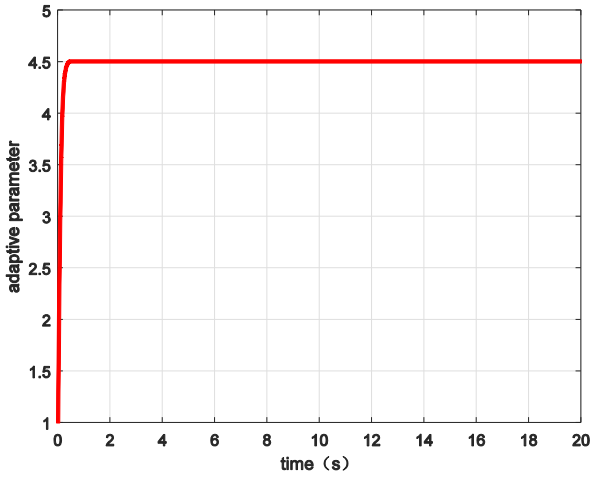

Figure 6. Adaptive parameter $\hat{K}_1$.

It can be seen in Figures 3–5 that the position and velocity can be tracked well in spite of the lumped disturbance and unknown uncertainties. The tracking error reached and remained on the SS and asymptotically converged to 0 along the SS.

For comparison, the NERL in [23] and the NRL in [24] are described by Eq. (30) and Eq. (31).

$$\dot{s} = -\frac{k_1}{N_1(s)}\mathrm{sgn}(s), k_1 > 0 \tag{30}$$

$$\dot{s} = -k_2 |X|^2 \mathrm{sgn}(s) - k_3 s, k_2, k_3 > 0 \tag{31}$$

where $N_1(s) = \partial + (1+\partial)e^{-\varepsilon_1 |s|^{p_1}}, \partial \in (0,1)$. As can be seen in Figure 6, the estimated value of the adaptive parameter tended to $\hat{K}_1 = 4.5$. Therefore, the simulation parameters of the reaching law in [24] were set as $k_1 = \hat{K}_1 = 4.5$, $\partial = 0.5$, $\varepsilon_1 = 1$, $p_1 = 1$, $k_2 = 1$ and $k_3 = 5$. Then, the comparative simulations are shown in Figures 7–9.

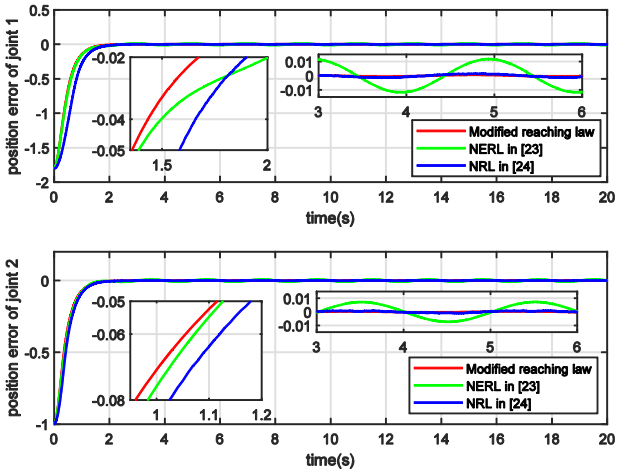

Figure 7. Two-joint position tracking error via different methods.

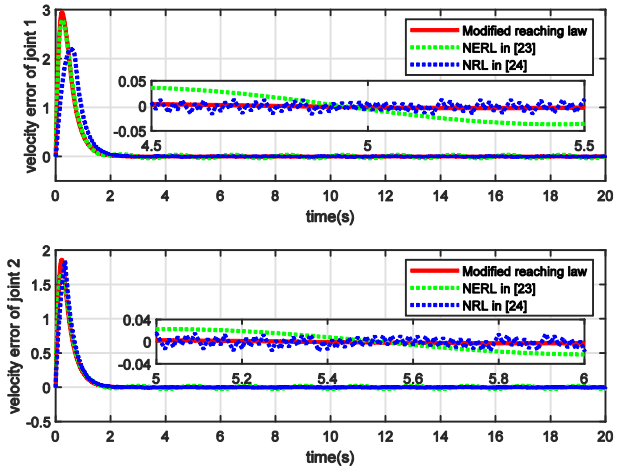

Figure 8. Two-joint velocity tracking error via different methods.

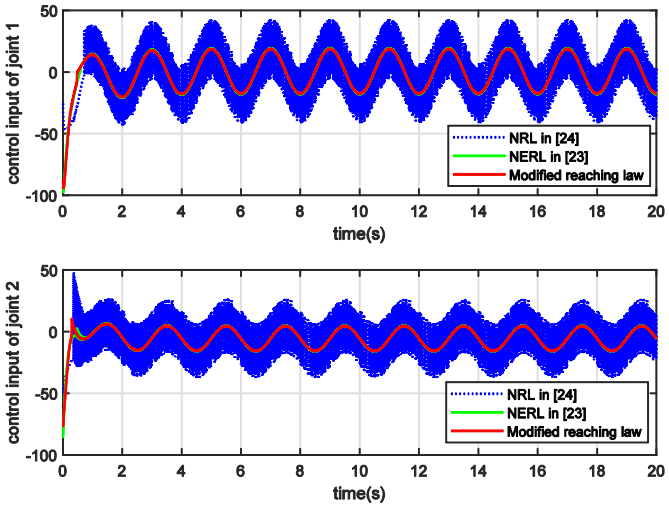

Figure 9. Two-joint control input via different methods.

As can be seen, the comparison simulations of the position and velocity tracking errors of the two joints, which were achieved using the related methods, are depicted in Figures 7–8. It is clear that, as compared to the controller that used the NERL from [23] and the NRL from [24], the position tracking was faster and more efficient; furthermore, the velocity tracking chattering was reduced with the current controller design. Figure 9 shows the comparison results for the control inputs of the two joints; it shows that the chattering of the control input was reduced under the conditions of the modified reaching law.

Moreover, to further verify the advantages of the modified reaching law, the signum function of the reaching law in [24] was replaced by the hyperbolic tangent function. The results of the considered comparison simulations are shown in Figures 10–11, and Figure 12 provides the curves for the control input signals. It can be seen that the NRL method from [24] resulted in less chattering, but the effect achieved by the proposed modified reaching law was better.

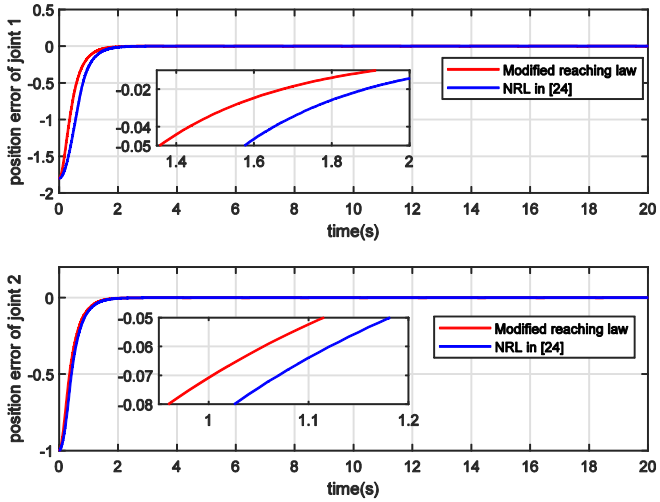

Figure 10. Two-joint position tracking error.

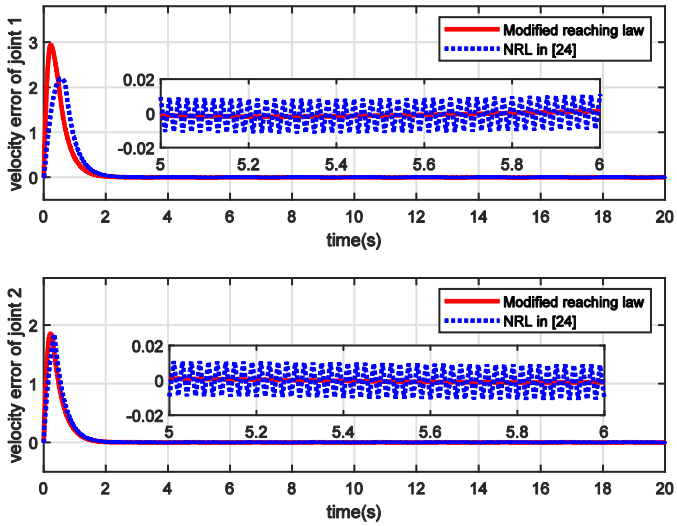

Figure 11. Two-joint velocity tracking error.

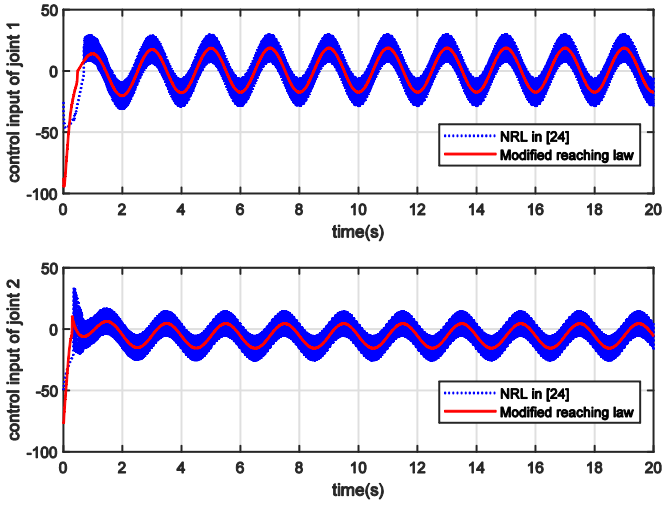

Figure 12. Two-joint control input.

Furthermore, the energy consumption (EC) of a plant is a key performance index in practice, and the formula of EC is as below.

$$\mathrm{EC} = \int_0^{t_r} u^2 dt \,. \tag{32}$$

Then, Table 1 shows the comparison results for the EC. The control method based on the current reaching law resulted in less energy loss than the methods proposed in [23] and [24].

Table 1. EC comparison results.

Control method	EC of Joint 1	EC of Joint 2
Proposed method	4412.7768	1962.5625
The method in [23]	4555.5988	1975.5307
The method in [24]	13511.2920	9898.1141
The method in [24] using tanh-function	7208.9799	4590.9251

Lastly, the following performance indexes, i.e., the integral squared error (ISE), integral absolute error (IAE) and integral time multiplied absolute error (ITAE) were also introduced from [28]. The values of these indexes, and the settling time (ST), are shown in Table 2; they were used to analyze the transient and steady performance of the manipulator.

$$\begin{cases} ISE = \int_0^{t_f} e^2(t)dt \\ IAE = \int_0^{t_f} |e(t)|dt \\ ITAE = \int_0^{t_f} t|e(t)|dt \end{cases}, \tag{33}$$

where t_f is the simulation time. From Table 2, it can be seen that the controller based on the modified adaptive reaching law more accurately tracked with a faster convergence.

Table 2. Performance indices of tracking response characteristics.

Control method	Joint	ISE	IAE	ITAE	ST
Proposed method	1	0.9530	0.2688	0.3910	1.357
	2	0.2688	0.2688	0.2046	1.115
The method in [23]	1	0.9806	1.0149	1.8104	1.389
	2	0.2811	0.5401	1.0826	1.126
The method in [24]	1	1.4739	1.2006	0.6805	1.583
	2	0.3239	0.5129	0.3032	1.179
The method in [24] using tanh-function	1	1.4739	1.1907	0.5709	1.576
	2	0.3239	0.5053	0.2172	1.181

6. Conclusion

In this study, a new adaptive modified reaching law was developed to improve the tracking performance and reduce the chattering of the plant. Then, a novel adaptive SMC was developed for robot manipulators with external disturbances and unknown uncertainties to automatically adapt the plant parameters and improve the performance of the system; the DO and the modified reaching law approach were applied. Through simulation experiments, the developed adaptive reaching law-based controller was demonstrated to accelerate the convergence speed, reduce the chattering and EC and enhance the robustness of the plant.

In the future, finite-time DO-based SMC methods can be studied to enable the realization of fast compensation and the improvement of the transient performance of the plant; additionally, some complex issues in practical control systems, such as cases in which there is a dead zone, input saturation, etc., may also be explored by using the proposed method.

Acknowledgments

This work was supported by the National Natural Science Foundation of China under grant number 61803217.

Conflict of interest

The authors declare that there is no conflict of interest.

References

1. C. Yang, Y. Jiang, W. He, J. Na, Z. Li, B. Xu, Adaptive parameter estimation and control design for robot manipulators with finite-time convergence, *IEEE Trans. Ind. Electron.*, **65** (2018), 8112–8123. https://doi.org/10.1109/TIE.2018.2803773
2. H. Wang, Adaptive control of robot manipulators with uncertain kinematics and dynamics, *IEEE Trans. Autom. Control*, **62** (2017), 948–954. https://doi.org/10.1109/TAC.2016.2575827
3. Y. Hu, J. Li, Y. Chen, Q. Wang, C. Chi, H. Zhang, et al., Design and control of a highly redundant rigid-flexible coupling robot to assist the COVID-19 oropharyngeal-swab sampling. *IEEE Robot. Autom. Lett.*, **7** (2022), 1856–1863. https://doi.org/10.1109/lra.2021.3062336
4. Y. Hu, H. Su, J. Fu, H. R. Karimi, G. Ferrigno, E. D. Momi, et al., Nonlinear model predictive control for mobile medical robot using neural optimization, *IEEE Trans. Ind. Electron.*, **68** (2021), 12636–12645. https://10.1109/TIE.2020.3044776
5. S. Mobayen, F. Tchier, L. Ragoub, Design of an adaptive tracker for n-link rigid robotic manipulators based on super-twisting global nonlinear sliding mode control, *Int. J. Syst. Sci.,* **48** (2017), 1990–2002. https://doi.org/10.1080/00207721.2017.1299812
6. A. Abooee, M. M. Khorasani, M. Haeri, Finite time control of robotic manipulators with position output feedback, *Int. J. Robust Nonlinear Control*, **27** (2017), 2982–2999. https://doi.org/10.1002/rnc.3721
7. R. J. Wai, R. Muthusamy, Fuzzy-neural-network inherited sliding-mode control for robot manipulator including actuator dynamics, *IEEE Trans. Neural Networks Learn. Syst.*, 24 (2013), 274–287. https://doi.org/10.1109/TNNLS.2012.2228230
8. Z. Zhao, J. Yang, S. Li, Z. Zhang, L. Guo, Finite-time super-twisting sliding mode control for Mars entry trajectory tracking, *J. Franklin Inst.*, **352** (2015), 5226–5248. https://doi.org/10.1016/j.jfranklin.2015.08.022
9. V. I. Utkin, A. S. Poznyak, Adaptive sliding mode control with application to super-twist algorithm: Equivalent control method, *Automatica*, **49** (2013), 39–47. https://doi.org/10.1016/j.automatica.2012.09.008
10. Z. Liu, H. R. Karimi, J. Yu, Passivity-based robust sliding mode synthesis for uncertain delayed stochastic systems via state observer, *Automatica*, **111** (2020), 108596. https://doi.org/10.1016/j.automatica.2019.108596
11. Z. Liu, J. Yu, H. R. Karimi, Adaptive H∞ sliding mode control of uncertain neutral-type stochastic systems based on state observer, *Int. J. Robust Nonlinear Control*, 30 (2020), 1141–1155. https://doi.org/10.1002/rnc.4817
12. T. Gonzalez, J. A. Moreno, L. Fridman, Variable gain super-twisting sliding mode control, *IEEE Trans. Autom. Control*, **57** (2012), 2100–2105. https://doi.org/10.1109/TAC.2011.2179878

13. X. L. Tang, Z. Liu, Sliding mode observer-based adaptive control of uncertain singular systems with unknown time-varying delay and nonlinear input, *ISA Trans.*, (2021), in press. https://doi.org/10.1016/j.isatra.2021.09.011
14. B. Jiang, C. C. Gao, Decentralized adaptive sliding mode control of large-scale semi-Markovian jump interconnected systems with dead-zone input, *IEEE Trans. Autom. Control*, (2021), in press. https://doi.org/10.1109/TAC.2021.3065658
15. H. R. Karimi, A sliding mode approach to H_∞ synchronization of master-slave time-delay systems with Markovian jumping parameters and nonlinear uncertainties, *J. Franklin Inst.*, **349** (2012), 1480–1496. https://doi.org/10.1016/j.jfranklin.2011.09.015
16. H. Liu, X. Tian, G. Wang, T. Zhang, Finite-time H-infinity control for high-precision tracking in robotic manipulators using backstepping control, *IEEE Trans. Ind. Electron.*, **63** (2016), 5501–5513. https://doi.org/10.1109/TIE.2016.2583998
17. S. Li, Z. Shao, Y. Guan, A dynamic neural network approach for efficient control of manipulators, *IEEE Trans. Syst., Man, Cybern.: Syst.*, **49** (2017), 1–10. https://doi.org/10.1109/TSMC.2017.2690460
18. A. Mohammadi, M. Tavakoli, H. J. Marquez, F. Hashemzadeh, Nonlinear disturbance observer design for robotic manipulators, *Control Eng. Pract.*, **21** (2013), 253–267. https://doi.org/10.1016/j.conengprac.2012.10.008
19. S. Yu, X. Yu, B. Shirinzadeh, Z. Man, Continuous finite-time control for robotic manipulators with terminal sliding mode, *Automatica*, **41** (2005), 1957–1964. https://doi.org/10.1016/j.automatica.2005.07.001
20. J. Baek, M. Jin, S. Han, A new adaptive sliding-mode control scheme for application to robot manipulators, *IEEE Trans. Ind. Electron.*, **63** (2016), 3628–3637. https://doi.org/10.1109/TIE.2016.2522386
21. H. Liu, J. Sun, J. Nie, L. Zou, Observer-based adaptive second-order non-singular fast terminal sliding mode controller for robotic manipulators, *Asian J. Control*, **23** (2020), 1845–1854. https://doi.org/10.1002/asjc.2369
22. W. Gao, J. C. Hung, Variable structure control of nonlinear systems: A new approach, *IEEE Trans. Ind. Electron.*, **40** (1993), 45–55. https://doi.org/10.1109/41.184820
23. A. Wang, X. Jia, S. Dong, A new exponential reaching law of sliding mode control to improve performance of permanent magnet synchronous motor, *IEEE Trans. Magn.*, **49** (2013), 2409–2412. https://doi.org/10.1109/TMAG.2013.2240666
24. C. J. Fallaha, M. Saad, H. Y. Kanaan, K. Al-Haddad, Sliding-mode robot control with exponential reaching law, *IEEE Trans. Ind. Electron.*, **58** (2011), 600–610. https://doi.org/10.1109/TIE.2010.2045995
25. Z. Zhao, H. Gu, J. Zhang, G. Ding, Terminal sliding mode control based on super-twisting algorithm, *J. Syst. Eng. Electron.*, **28** (2017), 145–150. https://doi.org/10.21629/JSEE.2017.01.16
26. W. H. Chen, D. J. Ballance, P. J. Gawthrop, J. O'Reilly, A nonlinear disturbance observer for robotic manipulators, *IEEE Trans. Ind. Electron.*, **47** (2000), 932–938. https://doi.org/10.1109/41.857974
27. S. Rajendran, D. Jena, Variable speed wind turbine for maximum power capture using adaptive fuzzy integral sliding mode control, *J. Mod. Power Syst. Clean Energy*, **2** (2014), 114–125. https://doi.org/10.1007/s40565-014-0061-3

28. N. M. Moawad, W. M. Elawady, A. Sarhan, Development of an adaptive radial basis function neural network estimator-based continuous sliding mode control for uncertain nonlinear systems, *ISA Trans.*, **87** (2018), 200–216. https://doi.org/10.1016/j.isatra.2018.11.021

AIMS Press